HAMILTON, W. C. (1965*b*). *Acta Cryst.* **18**, 502–510.
HUDSON, B. & MOSELEY, P. T. (1976). *J. Solid State Chem.* **19**, 383–389.
International Tables for X-ray Crystallography (1974). Vol. IV. Birmingham: Kynoch Press.
RICHESSON, M., MORRISON, L., COHEN, J. B. & PAAVOLA, K. (1971). *J. Appl. Cryst.* **4**, 524–527.
ROTH, W. L. (1975). *Crystal Structure and Chemical Bonding in Inorganic Chemistry*, edited by C. J. M. ROOYMANS & A. RABENAV, pp. 85–102. Amsterdam: North-Holland.
SARDI, O. (1969). PhD Thesis, Univ. of Indiana.
SCHWARTZ, L. H. & COHEN, J. B. (1977). *Diffraction from Materials*, pp. 191–192. New York: Academic Press.
SMITH, D. K. & NEWKIRK, H. W. (1965). *Acta Cryst.* **18**, 983–991.
STEELE, D. & FENDER, B. E. F. (1974). *J. Phys. C*, 7, 1–11.
TEUFER, G. (1962). *Acta Cryst.* **15**, 1187.
TOKONAMI, M. (1965). *Acta Cryst.* **19**, 486.
WILLIS, B. T. M. & PRYOR, A. W. (1975). *Thermal Vibrations in Crystallography*, pp. 142–159. London: Cambridge University Press.

Acta Cryst. (1979). A**35**, 795–802

Intensity Errors due to Beam Inhomogeneity and Imperfectly Spherical Crystals

BY H. D. FLACK AND M. G. VINCENT

Laboratoire de Cristallographie aux Rayons X, 24, quai Ernest Ansermet, Université de Genève, CH-1211 Genève 4, Switzerland

(*Received* 19 *February* 1979; *accepted* 28 *March* 1979)

Abstract

An analysis of the intensity errors from imperfectly spherical crystals with an inhomogeneous incident X-ray beam is presented. The crystals are considered to have either no absorption or strong absorption. The inhomogeneity of the incident beam profile is represented by three possible models: (*a*) a Lorentzian, (*b*) a Gaussian and (*c*) a second-order Taylor series expansion. The results are compared with intensities for electron density studies from five crystals.

1. Introduction

The necessity for precise intensity measurements of X-rays diffracted by a crystal has increased with the interest in electron density studies. The conditions which must be met to obtain useful results from metallic systems are more restrictive than those in light atom systems due to the presence of absorption in the material. A common approach to reducing systematic errors in heavy-atom systems is to try to prepare a sample in the form of a sphere. However, the shapes of crystals obtained are seldom truly spherical. In a previous publication (Vincent & Flack, 1979*a*), we have estimated the intensity variations among equivalent reflections due to absorption to be expected from imperfectly spherical crystals. The predicted intensity variations seem to be smaller than those currently obtained in a real experiment. We have thus been drawn to analyse the effects due to beam inhomogeneity and crystal miscentring jointly with absorption from imperfectly spherical crystals.

2. Relationship between intensity and shape variations

In order to investigate changes in diffracted intensity due to variations in shape, we need to calculate the total intensity (energy) diffracted by a crystal of given shape and then derive intensity changes for changes in shape. The integrated reflection intensity, ρ, from an infinitesimally small block of volume δV of a crystal is given by

$$\rho = Q\,\delta V, \tag{1}$$

where Q contains the Lorentz–polarization factors, structure amplitude squared and some fundamental physical constants (*International Tables for X-ray Crystallography*, 1967). ρ is related to the total amount of energy diffracted (E) by

$$\rho = E\omega/I_0, \tag{2}$$

where ω is the angular velocity of rotation of the crystal and I_0 is the intensity of the incident X-radiation falling normally on unit area per unit time. Combining (1) and (2) we find

$$E = (Q/\omega)\, I_0\, \delta V. \tag{3}$$

For a particular reflection under fixed measuring conditions, Q/ω is a constant. The total energy diffracted by a finite crystal may be obtained by

0567-7394/79/050795-08$01.00

integrating (3) in the kinematical approximation (loss of energy in the incident beam due to diffraction assumed negligible) to give

$$E_{\text{crystal}} = (Q/\omega) \int_V I_0 \, \mathrm{d}V. \tag{4}$$

A more useful property here is the total energy diffracted per unit volume of the crystal (φ); thus

$$\varphi = (Q/\omega)\frac{1}{V} \int_V I_0 \, \mathrm{d}V, \tag{5}$$

where V is the volume of the crystal.

To apply (5) to the prediction of intensity variations of imperfectly spherical crystals in an inhomogeneous beam, we proceed as follows. Consider a (perfectly) spherical crystal of radius R. For a non-absorbing sample, (5) may be applied directly to obtain the total diffracted intensity per unit volume as a function of R, *viz* $\varphi(R)$. Differentiating φ with respect to R, we find the change in intensity $\delta\varphi$ for a change in radius δR. However, as φ is a measure of diffracted intensity *per unit volume*, δR is an approximation to a change at constant volume and may thus be usefully interpreted as a measure of a change in shape rather than a change in volume. In this sense δR measures the scatter in the radii of the deformed sphere. Hence we have

$$\delta\varphi = \frac{\mathrm{d}\varphi}{\mathrm{d}R}\,\delta R. \tag{6}$$

As the relative errors of φ and R are of more interest experimentally, (6) may be rearranged to give,

$$\frac{\delta\varphi}{\varphi} = \left(\frac{R}{\varphi}\frac{\mathrm{d}\varphi}{\mathrm{d}R}\right)\frac{\delta R}{R}. \tag{7}$$

To emphasize that $\delta\varphi$ and δR are related to experimental variations, we now write them as σ_φ and σ_R to give

$$\sigma_\varphi/\varphi = \left(\frac{R}{\varphi}\frac{\mathrm{d}\varphi}{\mathrm{d}R}\right)\sigma_R/R, \tag{8a}$$

or

$$\beta = -(\sigma_\varphi/\varphi)/(\sigma_R/R) = \frac{-R}{\varphi}\frac{\mathrm{d}\varphi}{\mathrm{d}R}. \tag{8b}$$

β thus measures the relative intensity error with respect to the relative radius error. (5) and (8) are the basic equations to be applied to a model of the incident beam.

3. Models of the incident beam

A suitable functional representation of the beam incident upon the sample has to be chosen. We have chosen three simple models which may be used to represent the incident beam of our measuring apparatus. Vincent & Flack (1979*b*) give the X-ray intensity measured at the counter through a pinhole at the sample position for several radiations monochromatized by the 002 reflection of graphite on a commercial four-circle diffractometer. An analysis of the beam shape is given by Vincent & Flack (1979*b*). In the horizontal direction (x axis) the beam is very broad, whereas a definite peak is observable in the vertical (y axis) direction. We have chosen to represent this situation by the product of two functions, one of which, dependent only on x, is a constant, whilst the other, dependent only on y is a Lorentzian curve, or a Gaussian curve or a shape which may be represented by a second-order Taylor expansion about the origin. Thus

$$I_l = a_l/[b^2 + (y-c)^2], \tag{9a}$$

$$I_g = (a_g/\sigma\sqrt{2\pi}) \exp[-(y-c)^2/2\sigma^2], \tag{9b}$$

$$I_t = I(0) + yI'(0) + \frac{y^2}{2} I''(0), \tag{9c}$$

where c represents the peak position, and for the Lorentzian (9*a*), $a_l b^{-2}$ is the peak height and $2b$ the full width at half height, whereas for the Gaussian, $a_g/\sigma\sqrt{2\pi}$ is the peak height, σ represents the standard deviation of the profile and the full width at half height is $2{\cdot}354\sigma$. The units of b, c, σ and y are those of length and the units of a_l and a_g are chosen so that I_l and I_g will be the energy of X-radiation falling normally on unit area per unit time. For convenience we define

$$\varepsilon_l = R/b, \quad \eta_l = c/b, \quad \varepsilon_g = R/\sigma \quad \text{and} \quad \eta_g = c/\sigma, \tag{10}$$

where R is the radius of the crystal under consideration. Thus ε and η are respectively relative measures of the size of the crystal and of the beam miscentring with respect to the incident beam width. Where the context makes it clear which type of beam profile is being considered, the subscripts on ε_l, ε_g, η_l and η_g will be dropped. Our subsequent analysis will also assume that the beam is non-divergent. This makes the models, of course, somewhat crude but they are some of the simplest with the essential property that we wish to investigate, that of being inhomogeneous.

The Taylor series expansion has been included to produce simplified forms of the error estimates for the Lorentzian and Gaussian profiles, valid for small parameter values. This allows ready calculation and shows clearly the expected shapes of the error curves. Further, the Taylor series expansion produces formulae, suitable for any functional representation of the beam profile, which do not contain any integrals needing to be evaluated.

4. Intensity error calculations

In the following section, the models of the incident X-ray beam outlined above will be applied in the

calculation of intensity errors for some cases that are of experimental interest and that we have found to be amenable to analytical or numerical evaluation.

4(*a*) *Case of inhomogeneous beam and imperfectly spherical crystal with no absorption*

Substituting (9) into (5) we obtain

$$\varphi_l = (aQ/\omega)\frac{1}{V}\int_V \frac{dV}{b^2+(y-c)^2}, \tag{11a}$$

$$\varphi_g = (aQ/\omega)(1/\sigma\sqrt{2\pi})\frac{1}{V}\int_V \exp\left[-\frac{(y-c)^2}{2\sigma^2}\right]dV, \tag{11b}$$

$$\varphi_t = (Q/\omega)\frac{1}{V}\int_V [I(0)+yI'(0)+(y^2/2)I''(0)]\,dV. \tag{11c}$$

As the incident beam intensity is constant at constant y, we may perform the integration in (11) by cutting the crystal up into circular discs perpendicular to y as shown in Fig. 1. Thus with $V=\frac{4}{3}\pi R^3$, $dV=\pi r^2\,dy$, and $r^2=R^2-y^2$, (11) becomes

$$\varphi_l = (aQ/\omega)\frac{3}{4R^3}\int_{-R}^{R}\frac{R^2-y^2}{b^2+(y-c)^2}\,dy, \tag{12a}$$

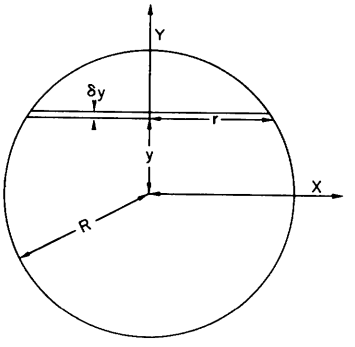

Fig. 1. Diffraction geometry for the case of an inhomogeneous beam and imperfectly spherical crystal with no absorption.

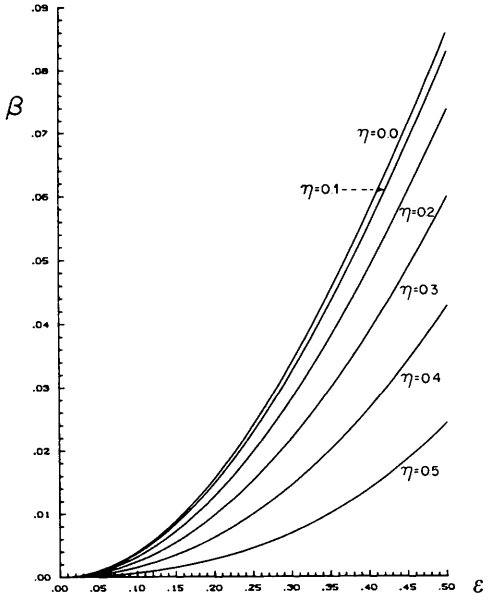

Fig. 2. Curves of β as a function of ε at fixed values of η. Case of a non-absorbing imperfectly spherical crystal in an inhomogeneous beam with a Lorentzian profile.

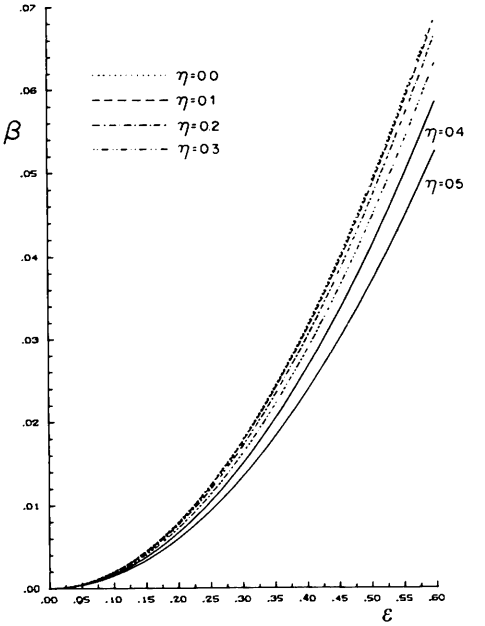

Fig. 3. Curves of β as a function of ε at fixed values of η. Case of a non-absorbing imperfectly spherical crystal in an inhomogeneous beam with a Gaussian profile.

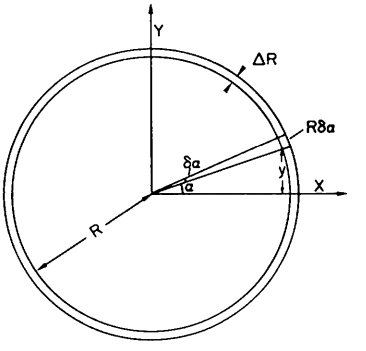

Fig. 4. Diffraction geometry for the case of an inhomogeneous beam and imperfectly spherical crystal with strong absorption and Bragg reflection at $\theta = 0°$.

$$\varphi_g = \left(\frac{aQ}{\omega}\right)\left(\frac{1}{\sigma\sqrt{2\pi}}\right)\frac{3}{4R^3} \times \int_{-R}^{R} (R^2 - y^2)\exp\left[-\frac{(y-c)^2}{2\sigma^2}\right]dy, \qquad (12b)$$

$$\varphi_l = (Q/\omega)\frac{3}{4R^3}\int_{-R}^{R} [I(0) + yI'(0) + (y^2/2)I''(0)] \times (R^2 - y^2)\,dy. \qquad (12c)$$

Performing the integral in (12*a*), followed by substitution in (8) one obtains

$$\beta_l = \frac{6\varepsilon - (\varepsilon^2 - 3\eta^2 + 3)[\arctan(\varepsilon+\eta) + \arctan(\varepsilon-\eta)] + 3\eta \ln\left[\frac{1+(\varepsilon-\eta)^2}{1+(\varepsilon+\eta)^2}\right]}{2\varepsilon - (\varepsilon^2 - \eta^2 + 1)[\arctan(\varepsilon+\eta) + \arctan(\varepsilon-\eta)] + \eta \ln\left[\frac{1+(\varepsilon-\eta)^2}{1+(\varepsilon+\eta)^2}\right]}, \qquad (13)$$

where ε and η are defined by (10). Fig. 2 shows β plotted as a function of ε at various values of η.

The integral in (12*b*), followed by substitution in (8), which involves a differentiation, were carried out numerically by Simpson's rule and with the approximation

$$\frac{d\varphi}{dR} \simeq \frac{\Delta\varphi}{\Delta R}, \quad \Delta R = 0{\cdot}001R.$$

Fig. 3 shows β as a function of ε at various values of η.

Evaluating the integral in (12*c*), followed by substitution in (8), one obtains

$$\beta_t = \frac{-R^2 I''(0)}{5I(0)}. \qquad (14)$$

Equation (14) may be used to check the results for β_l and β_g.

For a Lorentzian and a Gaussian, we obtain respectively from (9*a*) and (9*b*)

$$\frac{I''(0)}{I(0)} = -\frac{2}{b^2}\frac{(1-3\eta^2)}{(1+\eta^2)^2}, \qquad (15a)$$

$$\frac{I''(0)}{I(0)} = -\frac{1}{\sigma^2}(1-\eta^2), \qquad (15b)$$

and hence

$$\beta_l = \frac{2\varepsilon^2(1-3\eta^2)}{5(1+\eta^2)^2}, \qquad (16a)$$

$$\beta_g = \tfrac{1}{5}\varepsilon^2(1-\eta^2), \qquad (16b)$$

which are valid for small values of ε only. Equations (16) do however predict the quadratic behaviour of β as a function of ε seen in Figs. 2 and 3.

4(*b*) *Case of inhomogeneous beam and imperfectly spherical crystal with strong absorption and reflection at* $\theta = 0$

We may again use (11). We further assume that the absorption is so strong that diffraction can only take place from the surface of the pseudosphere. Under this restriction we may approximate the diffracting volume of the crystal to a ring in the x–y plane of width ΔR and thickness Δz. This is shown in Fig. 4.

Thus we have

$$V = 2\pi R\,\Delta R\,\Delta z, \quad dV = R\,\Delta R\,\Delta z\,d\alpha$$

and $\quad y = R\sin\alpha$

and substituting in (11) we obtain

$$\varphi_l = (aQ/\omega)\frac{1}{\pi}\int_{-\pi/2}^{\pi/2}\frac{d\alpha}{b^2 + (R\sin\alpha - c)^2}, \qquad (17a)$$

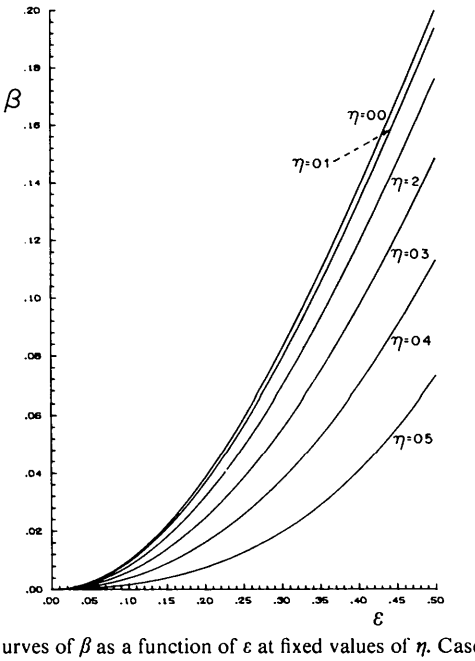

Fig. 5. Curves of β as a function of ε at fixed values of η. Case of a strongly absorbing imperfectly spherical crystal in an inhomogeneous beam with a Lorentzian profile and Bragg angle $\theta = 0°$.

$$\varphi_g = (aQ/\omega)(1/\sigma\sqrt{2\pi})(1/\pi) \times \int_{-\pi/2}^{\pi/2} \exp - \frac{(R\sin\alpha - c)^2}{2\sigma^2}\,\mathrm{d}\alpha, \qquad (17b)$$

$$\varphi_t = (Q/\omega)\frac{1}{\pi}\int_{-\pi/2}^{\pi/2} [I(0) + RI'(0)\sin\alpha + \tfrac{1}{2}R^2 I''(0)\sin^2\alpha]\,\mathrm{d}\alpha. \qquad (17c)$$

When $c = 0$, integration of (17a) and substitution in (8) gives

$$\beta_l = \frac{\varepsilon^2}{1+\varepsilon^2}. \qquad (18)$$

In the general case of $c \neq 0$, integration of (17a) and (17b) followed by differentiation in (8) were carried out numerically as in case 4(a). The curves of β as a function of ε are shown in Figs. 5 and 6. Equation (17c) yields

$$\beta_t = \frac{-R^2}{2}\frac{I''(0)}{I(0)}, \qquad (19)$$

which for small values of ε gives

$$\beta_l = \varepsilon^2\frac{(1-3\eta^2)}{(1+\eta^2)^2}, \qquad (20a)$$

and

$$\beta_g = \frac{\varepsilon^2}{2}(1-\eta^2), \qquad (20b)$$

by use of (15).

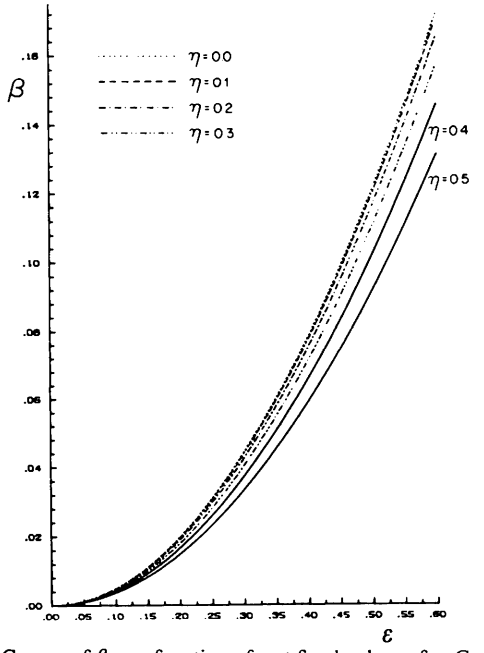

Fig. 6. Curves of β as a function of ε at fixed values of η. Case of a strongly absorbing imperfectly spherical crystal in an inhomogeneous beam with a Gaussian profile and Bragg angle $\theta = 0°$.

4(*c*) *Case of inhomogeneous beam and imperfectly spherical crystal with strong absorption and reflection at* $\theta = \pi/2$

Again we use (11). With strong absorption at $\theta = \pi/2$, we assume the diffracting volume of the crystal to be a spherical surface shell of uniform thickness Δz, as shown in Fig. 7. Thus we have

$$V = \pi R^2\,\Delta z, \quad \mathrm{d}V = \mathrm{d}x\,\mathrm{d}y\,\Delta z, \quad r^2 = R^2 - y^2,$$

and substituting in (11) we obtain

$$\varphi_l = (aQ/\omega)\frac{2}{\pi R^2}\int_{-R}^{R}\int_{0}^{r}\frac{1}{b^2+(y-c)^2}\,\mathrm{d}x\,\mathrm{d}y = (aQ/\omega)\frac{2}{\pi R^2}\int_{-R}^{R}\frac{(R^2-y^2)^{1/2}}{b^2+(y-c)^2}\,\mathrm{d}y, \qquad (21a)$$

$$\varphi_g = (aQ/\omega)(1/\sigma\sqrt{2\pi})(2/\pi R^2) \times \int_{-R}^{R}(R^2-y^2)^{1/2}\exp\left[-\frac{(y-c)^2}{2\sigma^2}\right]\mathrm{d}y, \qquad (21b)$$

$$\varphi_t = (Q/\omega)\frac{2}{\pi R^2}\int_{-R}^{R}[I(0) + yI'(0) + (y^2/2)I''(0)](R^2-y^2)^{1/2}\,\mathrm{d}y. \qquad (21c)$$

Equations (21a) and (21b) were evaluated numerically in the same way as case 4(a). The graphs of β are shown in Figs. 8 and 9. Evaluation of (21c) leads to

$$\beta = -\frac{R^2}{4}\frac{I''(0)}{I(0)}, \qquad (22)$$

which for small ε gives

$$\beta_l = \frac{\varepsilon^2}{2}\frac{(1-3\eta^2)}{(1+\eta^2)^2}, \qquad (23a)$$

and

$$\beta_g = \frac{\varepsilon^2}{4}(1-\eta^2), \qquad (23b)$$

by use of (15).

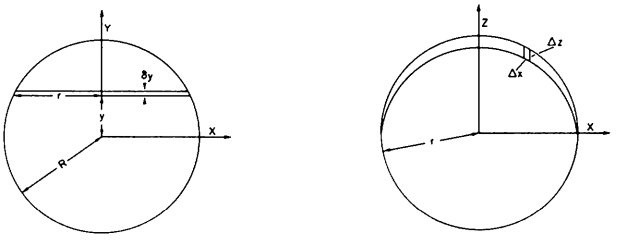

Fig. 7. Diffraction geometry for the case of an inhomogeneous beam and imperfectly spherical crystal with strong absorption and Bragg reflection at $\theta = 90°$.

4(*d*) *Case of a crystal wobbling in an inhomogeneous beam*

We assume a very small crystal which is moving linearly along y from $-d$ to $+d$. The mean total energy diffracted by the crystal is thus given by

$$\bar{\varphi} = (QV/\omega) \int_{-d}^{d} I_0(y)\,\mathrm{d}y \Big/ \int_{-d}^{d} \mathrm{d}y, \tag{24}$$

and the mean square total energy by

$$\overline{\varphi^2} = (Q^2 V^2/\omega^2) \int_{-d}^{d} I_0^2(y)\,\mathrm{d}y \Big/ \int_{-d}^{d} \mathrm{d}y. \tag{25}$$

The relative intensity variation may be written as

$$\sigma_I/I = [\overline{\varphi^2} - (\bar{\varphi})^2]^{1/2}/\bar{\varphi}, \tag{26}$$

and substituting (9), (24) and (25) into (26) we obtain

$$(\sigma_I/I)_l = [\arctan(\xi-\eta) + \arctan(\xi+\eta)]^{-1} \times \left\{ \frac{\xi(\xi-\eta)}{1+(\xi-\eta)^2} + \frac{\xi(\xi+\eta)}{1+(\xi+\eta)^2} + \xi[\arctan(\xi-\eta) + \arctan(\xi+\eta)] - [\arctan(\xi-\eta) + \arctan(\xi+\eta)]^2 \right\}^{1/2}, \tag{27a}$$

where $\xi_l = d/b$.

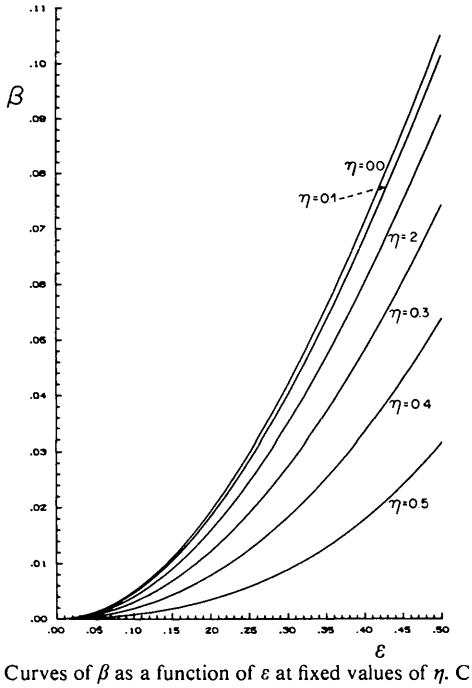

Fig. 8. Curves of β as a function of ε at fixed values of η. Case of a strongly absorbing imperfectly spherical crystal in an inhomogeneous beam with a Lorentzian profile and Bragg angle $\theta = 90°$.

For the Gaussian distribution the integrals were evaluated numerically by Simpson's rule with the substitution $\xi_g = d/\sigma$. Graphs of σ_I/I as a function of ξ and η are shown in Figs. 10 and 11. Equation (9*c*) leads to

$$(\sigma_I/I)_t = \left\{ \frac{1}{3}\left[d\frac{I'(0)}{I(0)}\right]^2 + \frac{1}{45}\left[d^2\frac{I''(0)}{I(0)}\right]^2 \right\}^{1/2}, \tag{27c}$$

valid for small values of d. From (27*c*) one obtains

$$(\sigma_I/I)_l = \left\{ \frac{4\xi^2\eta^2}{3(1+\eta^2)^2} + \frac{4\xi^4(1-3\eta^2)^2}{45(1+\eta^2)^4} \right\}^{1/2}, \tag{28a}$$

$$(\sigma_I/I)_g = \left\{ \frac{\xi^2\eta^2}{3} + \frac{\xi^4(1-\eta^2)^2}{45} \right\}^{1/2}. \tag{28b}$$

The approximate forms of σ_I/I in (28) show the change from quadratic to linear behaviour on increasing the value of η from 0.

5. Examples

The data given in Tables 1 and 2 are for crystals prepared for electron density studies. The intensities are of high quality and much more than the asymmetric region of reciprocal space has been measured. The alloy and oxide samples were ground to as near spherical in shape as could be obtained. This is not the case with the fumaric acid crystal which is as-grown and has well developed faces. The mean radius and its variance were estimated by measuring the distances between opposite corners and between opposite faces.

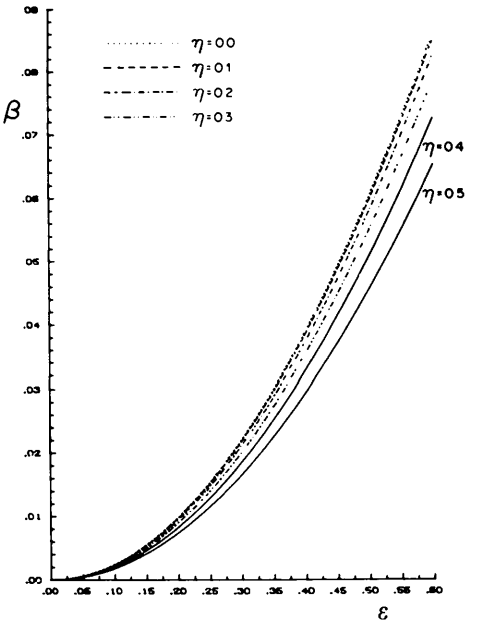

Fig. 9. Curves of β as a function of ε at fixed values of η. Case of a strongly absorbing imperfectly spherical crystal in an inhomogeneous beam with a Gaussian profile and Bragg angle $\theta = 90°$.

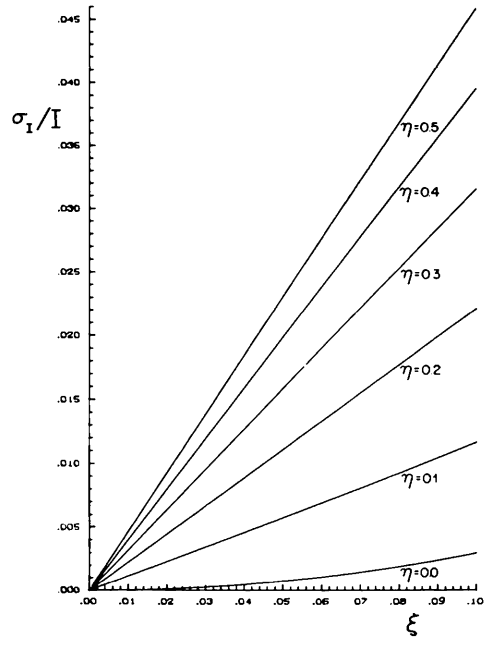

Fig. 10. Curves of σ_I/I as a function of ξ at fixed values of η. Case of a miscentred small crystal in an inhomogeneous beam with a Lorentzian profile.

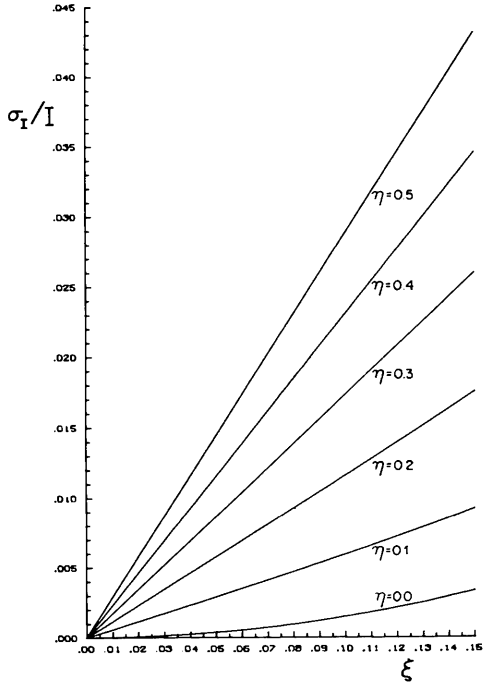

Fig. 11. Curves of σ_I/I as a function of ξ at fixed values of η. Case of a miscentred small crystal in an inhomogeneous beam with a Gaussian profile.

The measurements of the incident beam parameters were obtained as described by Vincent & Flack (1979*b*). The incident beam profile has a shape between a Lorentzian and a Gaussian. We have thus given in Table 2 error estimates based on both of these forms for comparison. The incident X-ray beam characteristics were measured at some time other than just prior to data collection and may thus be different from those operational during data measurements. This is particularly the case for the beam offset parameter, c, which is the distance between the optical centre of the diffractometer and the incident beam peak position in the vertical or y direction. On our machine the monochromator inclination, which is the primary adjustment affecting c, is controlled by a coarse adjusting system without an entirely satisfactory locking mechanism. Hence any mechanical vibration of a regular or impulse nature is likely to put the monochromator slightly out of adjustment. Further, in the method used to measure the incident beam profile it is difficult to define with precision the position of the optical centre. We have thus been pessimistic in our calculations of the intensity errors by using the value of η between 0 and the values given in Table 1 which gives the largest intensity error. Inspection of the curves in the figures shows that a value of $\eta = 0$ was used for the calculations of cases 4(*a*), (*b*) and (*c*) whereas the values of Table 1 were used for case 4(*d*).

The value of d used in the calculation of $\xi = d/b$ or d/σ for the wobbling crystal in an inhomogeneous beam is based on the optical resolution of the telescope used to centre the sample. One division of the grid of this telescope corresponds to 25 μm. If we suppose that the grid can be read to $\frac{1}{4}$ of a division in centring a crystal we obtain the value of d given in Table 1.

The intensity error due to the interplay of absorption and non-sphericity has been estimated by the method of Vincent & Flack (1979*a*). For the inhomogeneous beam coupled with a non-spherical crystal, we have calculated both the no absorption and the strong absorption cases for the ScSi and the oxide crystals as they probably represent some intermediate case. For fumaric acid, it seems irrelevant to give the strong absorption values. The values given in Table 2 were calculated from the formulae derived from the Taylor

Table 1. *Parameters defining the incident* X-*ray beam*

Full width at half height (mm)	1·0
Lorentzian parameter, b (mm)	0·5
Gaussian parameter, σ (mm)	0·42
Beam offset, c (mm)	0·125
Movement, $2d$ (mm), of crystal due to wobbling	0·013
η (Lorentzian) (c/b)	0·25
η (Gaussian) (c/σ)	0·29
ξ (Lorentzian) (d/b)	0·013
ξ (Gaussian) (d/σ)	0·015

Table 2. *Error calculations on five crystalline samples*

Compound		ScSi	Ti_2O_3	V_2O_3	V_2O_3	Fumaric acid
Radiation used		Mo $K\alpha$	Ag $K\alpha$	Ag $K\alpha$	Ag $K\alpha$	Mo $K\alpha$
Linear absorption coefficient (μ) mm^{-1}		5·203	3·680	4·467	4·467	0·072
Mean radius of the crystal R (mm)		0·025	0·079	0·131	0·079	0·128
Radius variation σ_R (mm)		0·0013	0·0008	0·0025	0·0025	0·038
σ_R/R (%)		5·1	0·95	1·91	3·16	29·4
μR		0·13	0·29	0·59	0·35	0·01
ε (Lorentzian) = R/b		0·05	0·16	0·26	0·16	0·26
ε (Gaussian) = R/σ		0·06	0·19	0·31	0·19	0·31
Error estimates (σ_I/I) (%)						
Absorption with aspherical crystal, $\theta = 0$; $\theta = 90°$		0·07; 0·06	0·04; 0·03	0·21; 0·16	0·17; 0·14	0·04; –
Aspherical crystal with:	inhomogeneous beam of profile:					
4(*a*) no absorption	Lorentzian; Gaussian	0·005; 0·004	0·01; 0·007	0·05; 0·04	0·03; 0·02	0·79; 0·56
4(*b*) strong absorption $\theta = 0°$	Lorentzian; Gaussian	0·01; 0·009	0·03; 0·02	0·13; 0·09	0·08; 0·06	–
4(*c*) strong absorption $\theta = 90°$	Lorentzian; Gaussian	0·006; 0·005	0·01; 0·009	0·07; 0·05	0·04; 0·03	–
4(*d*) wobbling crystal	Lorentzian; Gaussian	0·35; 0·25	0·35; 0·25	0·35; 0·25	0·35; 0·25	0·35; 0·25
Data intensity measurements						
Internal consistency factor J (%)		2·4	1·1	2·1	1·4	2·4
Number of reflections contributing to J		86	515	603	602	1127

series expansion of the incident beam, as the values of ε, η and ξ are quite small.

Finally in Table 2 we give values of the internal consistency factor J of the data set where J is defined by

$$J = \left[\sum_i \sum_k \left| I_{ik} - \left(\frac{\sum_l I_{il}}{n_l} \right) \right| \Big/ n_i \right] \Big/ \left[\sum_i \frac{\sum_l I_{il}}{n_i} \right],$$

$\sum_l I_{il}/n_i$ being the arithmetic mean of n_i symmetry-related reflections where $\sum_i$ is the sum over all reflections with $n_i \geq 2$.

The internal consistency values are for intensities corrected for the effect of extinction, if this was found to be significant in the crystal.

6. Discussion

The total experimental error for our intensity measurements should be obtained by taking the square root of the sum of the squares of the individual and supposedly independent errors. If we do this on our test crystals we obtain values considerably smaller than the internal consistency factor of the respective data sets even supposing worst case values (*i.e.* strong absorption at $\theta = 0°$ with a Lorentzian profile).

Looking at the contributions to the total error, we see that the wobbling crystal always produces a significant contribution to the intensity error despite our conservative estimate of the amount of wobble taking place. We have taken no account in our estimate of d of movements due to a lack of mechanical rigidity in the goniometer head, fibre or crystal support or to vibration of the crystal-supporting fibre due to turbulence from a stream of cold nitrogen gas. If the amount of wobble supposed to be taking place is doubled or tripled, the relative intensity errors increase proportionally and the total errors approach those found experimentally in the internal consistency factors. Hence with an inhomogeneous beam, mechanical instability in the goniometer head, fibre and crystal support can be important sources of error.

For our test samples it is only with the fumaric acid crystal that there is an important error contribution due to the interplay of beam inhomogeneity and non-sphericity of the crystal. The alloy and oxide crystals have been carefully prepared to be as nearly spherical as possible and our calculations show that there would be very little advantage in making them either smaller or more spherical.

The intensity errors may always be reduced with a more homogeneous beam of X-rays. One way of achieving this is to do away with the monochromator. For example, Coppens *et al.* (1974) now use only β-filtered radiation with the diffractometer working in the step-scan mode. It is clear from our calculations that such a technique should produce about a 1% diminution in the internal consistency factor of data from the fumaric acid crystal, and 0·35% from the oxide and alloy crystals. Moreover, the error reduction could be even higher if the amount of wobble has been seriously underestimated as suggested above.

This work was partially sponsored by the Swiss National Science Foundation under project No. 2.786-0.77 and 2.004-0.78.

References

COPPENS, P., ROSS, F. K., BLESSING, R. H., COOPER, W. F., LARSEN, F. K., LEIPOLDT, J. G., REES, B. & LEONARD, R. (1974). *J. Appl. Cryst.* **7**, 315–319.

International Tables for X-ray Crystallography (1967). Vol. II, p. 265. Birmingham: Kynoch Press.

VINCENT, M. G. & FLACK, H. D. (1979*a*). *Acta Cryst.* A**35**, 78–82.

VINCENT, M. G. & FLACK, H. D. (1979*b*). In preparation.